AADE-18-FTCE-030

Effects of Thermal Stresses on Cement Seal Integrity in OCS Wells

Nathan Pinkston PE and Alistair Gill PE, Wild Well Control; Paul Sonnier, N. Kyle Combs, and Larry T. Watters, CSI Technologies

Abstract

This paper quantifies potential for cement sealant failure under thermally induced stress, or thermal stress. Information is based on results of two BSEE-funded investigations of thermal stress gradients on well integrity in OCS wells. Emphasis on long-term well barrier durability and advancement of deepwater technology to realize deeper wells in deeper water depths are raising awareness of well integrity risks from thermal gradients created during OCS well construction and production. Goals of these investigations were to assess potential for thermally-induced failure and determine mitigation strategies.

The investigations covered physics of thermal stress magnitude and rate on well systems and individual well components, identified performance critical properties of cement sealants and other well components required to withstand thermal stresses, described failure mechanisms driven by thermal stresses, and highlighted importance of thermal stress as a well integrity design component. Extensive laboratory and large-scale physical modeling and numerical simulations covering the entire range of OCS well architecture and operations highlight the risk of sealant failure resulting from thermal stresses at various points along the well at various times.

Results of these studies quantified the sources and magnitudes of thermal gradients occurring in OCS wells. Analysis of physical and numerical modeling results quantified barrier failure potential for individual well component materials as well as integrated system durability. Comparative evaluation of cyclic thermal stresses on Portland cement sealants vs. design and performance properties identified thermal resistance gaps in design methodology that can be addressed through additional cement formulation and design effort.

Introduction

Cement seal integrity and durability is the root of constructing and maintaining a petroleum well as a secure, continuous conduit for producing hydrocarbon from a formation. This conduit must contain and isolate produced fluids. Additionally, the seals establish flow barriers to isolate or prevent unwanted fluid movement from non-productive formations. This closed conduit and barrier seal system enables controlled production over the operating life of the well including maintenance operations while preventing unwanted fluid migration or surface escape with associated contamination or environmental damage.

Seal establishment is often considered a “set it and forget it” operation occurring in a static environment. This is not the case. Cement sealant design and placement are complex processes seldom performed with 100% effectiveness. Well operations following cementing induce stresses to a casing-cement-formation system with sufficient frequency and of sufficient magnitude to damage seal integrity resulting in flow behind pipe or sustained casing pressure at wellhead (SCP). While cement seal failure is not the only cause of SCP, it is a significant one. Operationally, production occurs from the large majority of these wells with monitoring of SCP for increases or leaks. However, the barrier breaches revealed by SCP increase risk of emissions or well control issues. Over the past two decades, emphasis on well abandonment to effectively erase the existence of a wellbore further drives the importance of producing durable well seals.

This level of OCS wells with evidence of flow barrier problems provokes the question of cement seal durability under the thermal and mechanical stresses imposed by well operations. These stresses are induced by completion, remediation, and maintenance operations ranging from stimulation to production shut-in due to weather. Thermal gradients along well length are large and more complex as water depth increases. Pressure fluctuations are likewise large and increase with increasing water depth. Rates of change in stresses vary significantly. This complex well system coupled with multiple sources of cyclic stress do not support straightforward analytical solutions of seal durability.

This paper quantifies potential for cement sealant failure prediction under thermal stress. Information is based on results of two BSEE-funded investigations of thermally-induced stress gradients on well integrity in OCS wells. Goals of these investigations were to assess potential for thermally-induced failure, establish a reliable method of prediction and determine mitigation strategies.

Physics of thermal stress magnitude and rate of change on well systems and individual well components, critical performance properties of cement sealants and other well components required to withstand thermal stresses, and failure mechanisms driven by thermal stresses are assessed. Extensive laboratory and large-scale physical modeling and numerical simulations covering the entire range of OCS well architecture

and operations show significant risk of sealant failure can result from thermal stresses at various points along the well at various times.

Results of these studies quantify the sources and magnitudes of thermal gradients occurring in OCS wells. Analysis of physical and numerical modeling results quantify barrier failure potential for individual well component materials as well as integrated system durability. Comparative evaluation of cyclic thermal stresses on Portland cement sealants vs. design and performance properties identified thermal resistance gaps in design methodology that can be addressed through additional cement formulation and design effort.

The document outlines the project team and approach for an evaluation of the effects of thermal shock in OCS well bore integrity. Thermal shock refers to stresses induced by thermal gradients generated during well construction or operation. These thermally-induced stress gradients vary in magnitude and duration depending on operational cause, location in the well, and thermal properties of well materials. The well must withstand these stresses and remain a closed flow path for produced well fluids. Any breach of the conduit results in potential damage to personnel safety and the environment as well as loss of revenue and costly remediation. Thus, the importance of understanding thermal stress, potentially a significant threat to integrity imposed on a well bore, is vitally important to protecting the OCS environment and ensuring safe working conditions. Once the stresses of thermal stress are defined and bracketed, risk assessment of thermal stress generated by various well operations on well integrity will identify operational concerns and associated potential failure points in the well. From this, methods to improve well bore durability sufficiently to withstand stresses induced by thermal stress events can be evaluated.

OCS well integrity is a serious concern. Census of OCS well integrity issues in the Gulf of Mexico indicate that as many as 60% of wells operating today have sustained casing pressure "From Mud to Cement – Building Gas Wells (Article by Schlumberger in Oilfield Review Autumn 2003). SCP is an explicit indication of a well seal failure. Each one of these SCP instances results in cost to the operator to monitor or remediate the problem. Ultimately each instance indicates reduced well productivity. Even if a well is a commercial success and operates over its intended lifetime with SCP, that leak must finally be fixed when the well is abandoned.

The approach for this study builds on a recently-completed thermal stress-well durability study employing an integrated approach of fundamental understanding and problem definition, physical experimentation, and numerical modeling to assess the effects of stress generated on the integrated well system. This integrated well system, consisting of an array of telescoping steel casings sealed with Portland cement into a borehole drilled from the sea bed to the hydrocarbon reservoir, is extremely large and complicated. Operational failures during construction such as lost circulation or poor cement placement may produce a well that will not withstand thermal stresses even if it were originally designed properly. The approach outlined for this proposed project ties the fundamental materials science and thermodynamics of the system to integrity of a complex operating well. Mechanical and thermal properties of well components, well environment, and operating conditions are all considered. Results of the investigation and the methods developed therein allows assessment of thermal stress effects on a range of well systems and components. This approach allows meaningful assessment of risk to well integrity by thermal stress. From there, potential means of risk mitigation are assessed and compared. Thus, the investigative approach described here is designed to produce a method to assess potential risk for well integrity failure induced by thermal stress and to compare and contrast means to mitigate that risk.

Method

Mechanical Lab-Data

The literature review delivered two representative well descriptions for this study. The descriptions for these study wells are included below for reference in discussion of well conditions, casing-cement-formation system parameters, and stimulation effects. Information regarding bottom-hole treating pressure and bottom-hole temperature effects during typical hydraulic fracturing or frac pack treatments were added to this summary.

TABLE 1 WELL CONDITIONS FOR OCS WELL TYPES

Well Conditions	Deepwater, Shallow target	Deepwater, Deep target
BHT (°F)	155	250+
BHP (psi)	8000	17000
MD (ft)	14000	25600
TVD (ft)	13500	25000
Water Depth (ft)	5000	5000
Deviation (o)	25o	20o
Formation lithology	Sandstone, Shale	Sandstone, Shale
Formation properties	35% porosity	30% porosity
Production OH size (in)	12.250	12.25
Production Casing size (in)	9.875	9.625
Production Casing weight (lbs)	62.80	53.50
Production casing grade	Q-125	Q-125
Production tubing size (in)	4.50	3.50
Production tubing weight (lbs)	12.75	9.30
Production tubing grade	HYP 13 Cr	13 Cr 110 BTS-8
Completion type	Frac pack, Diesel	Frac pack, Matrix acid, Diesel
Completion fluid type	CaBr2, CaCl2	CaBr2, CaCl2
Completion fluid density (ppg)	11.80	15
Perforated section length (ft)	100	200
Number of completed stages	2	2
Treating Temperature Change(°F)	58oF Cooler	87oF Cooler
Change in bottom hole pressure	Bottom Hole Treating Pressure starts at 1000 psi above hydrostatic and builds to 3000 psi	
Frac thru casing or tubing	Frac thru tubing, packer set 100' above pay zone,	
Production string OH or cemented	Cemented	Cemented
Fracture treatment volumes (gal)	36,500	81,500

Fracture treatment rates (bpm)	30	40

Note that these designs, which are representative of those currently used by operators in OCS, are normal density and designed to minimize settling and free fluid. The mechanical properties of these systems are representative of standard cement compositions used for these applications.

Small Scale Physical Modeling

Wellbore stresses experienced during stimulation treatments were simulated in the lab to determine how temperature cycling during stimulation affects bond and seal integrity. Testing for conventional performance properties included Density, Rheology, Fluid Loss, Free Fluid, Thickening Time and Compressive Strength. Descriptions of these tests are found in Testing Methods and Mechanical Properties section. Testing also included mechanical property evaluation including compressive strength, tensile strength, Young's modulus and Poisson's Ratio. Coefficient of thermal expansion, heat capacity, and thermal conductivity were also measured for each cement as input for analysis of thermal cycling effects. A non-standard physical property, termed anelastic strain, was determined for each composition. This property describes the magnitude of plastic strain occurring due to cyclic stresses on the cement below the composition's elastic limit. These strains most likely occur due to micro-failure of cement pore structure. Evaluations of cement-pipe bond and seal durability of the cement seal of the casing-bore hole annulus were performed by shear bond testing and specialized annular seal testing.

Two cement compositions (resilient and low-density) were added to the Deepwater Shallow Target design scenario to broaden the testing beyond the basic cement compositions routinely employed. Resilient cement is used to reduce risk of cement mechanical failure. Chance of lost circulation can dictate the need for low-density cement. Both these compositions are designed to provide adequate handling time for placement, adequate fluid loss control, and to minimize settling and free fluid. Operators cementing an actual well may choose to design lower rheology depending on drilling fluid and spacer rheology as well as specific wellbore conditions. The mechanical properties of these systems are representative of the range of standard cement compositions used for these applications.

Mechanical and Thermal Properties

Mechanical properties of the test compositions were measured and are displayed in Table 3. Cement designs 1-6 in Table 2 and Table 3 are additional systems tested in the second investigation. Cement designs 1-3 represent conditions found in a Shelf well. Cement 1 is a lightweight surface lead, Cement 2 is a Top of Liner, and Cement 3 is a Production Liner. Cement designs 4-6 represent conditions found in a Deepwater well. Cement 4 is a Surface Lead, Cement 5 is a Liner Lead, and Cement 6 is a Foamed Production Tieback.

Overall results indicate that the cement systems generally exhibit superior performance than generic cements of similar density. Comparison of these data with those from previous studies indicate increased compressive strength, Young's modulus, tensile strength, impact strength and reduced anelastic strain. Overall, these results along with the design properties demonstrate that a focus of OCS cementing is maximizing cement quality.

TABLE 2 PROPERTIES OF SELECT DESIGNS

ID	TVD (ft)	Casing/Liner	Density (lb/gal)
Cement 1	4200	14 in Csg	12.0
Cement 2	12100	9 5/8 in Liner	17.0
Cement 3	16500	5 in Liner	13.5
Cement 4	4500	20 in Csg	16.4
Cement 5	6700	16 in Liner	13.5
Cement 6	17000	9 5/8 in Csg	16.4
Deepwater Shallow Target Conventional	13500	9 7/8 in Csg	16.4
Deepwater Shallow Target Low Density	13500	9 7/8 in Csg	13.0
Deepwater Shallow Target Resilient	13500	9 7/8 in Csg	15.9
Deepwater Deep Target	25000	9 5/8 in Csg	16.4

TABLE 3 MECHANICAL PROPERTIES OF SELECT DESIGNS

ID	Young's Modulus [psi]	Poisson's Ratio	Compressive Strength [psi]	Tensile Strength [psi]
Cement 1	3.18E5	0.26	448	69
Cement 2	2.20E6	0.26	6310	706
Cement 3	1.67E6	0.27	5044	571
Cement 4	1.11E6	0.21	1309	243
Cement 5	7.35E5	0.28	1858	253
Cement 6	1.67E6	0.27	10732	1114
Deepwater Shallow Target Conventional	2.34E6	0.27	6325	560
Deepwater Shallow Target Low Density	2.34E5	0.18	365	140
Deepwater Shallow Target Resilient	1.74E6	0.23	4485	500
Deepwater Deep Target	1.73E6	0.23	3205	385

Annular Seal Testing

Cement seal durability for each cement composition was evaluated in the laboratory via a small-scale procedure named annular seal testing. The method involved constructing a scaled-down wellbore system consisting of an inner pipe (casing) fitted into the center of a larger pipe which created an annulus. The material of the outer pipe, which represented the borehole wall, was varied to investigate effects of formation mechanical properties on seal performance. Cements were mixed, poured into the annuli of these test fixtures, and cured. After curing, gas pressure was applied at the bottom of the cemented annulus and thermal energy was applied to the system via the center pipe. The system was subjected to cyclic energy input until seal failure occurred. Cumulative energy required to

initiate gas flow was recorded along with position of gas flow first appearance in the annular space at the top.

It is important to note that failure is defined by actual establishment of gas flow through the cemented annulus. Mathematical analysis of failure induced in cement using only strength properties of the cement predicts failure always occurring at the inner pipe wall with lower energy input than observed. Testing in the laboratory with a range of cements, formation properties, and energy inputs produced a data set with which the aspects of the complex system can be compared.

Large-Scale Annular Seal

Schematics of the large-scale test fixtures for thermal testing are presented in Figure 1 below. For thermal testing, chilled water is circulated through the center pipe for 30 minutes followed by 30 minutes of circulating heated fluid. Thus a thermal differential of around 100°F can be applied to the inner casing-cement interface.

The cement was cured for 7 days at which time UCA tests indicated the composition developed compressive strength similar to that developed by the small-scale cement compositions cured 2 days at 140°F. Thus, mechanical properties of the cement systems in small and large scale tests were determined to be comparable.

After curing, the annular seal competence was confirmed by application of 20 psi gas pressure at the bottom of the annulus with no pressure increase occurring at the top of the annulus during the 1-hour test duration. Then, the inner pipe was filled with water and thermal cycling started. This cycle was controlled automatically and repeated continuously throughout the time each day that CSI's laboratory was manned. The data acquisition system logged temperature in the inner pipe, the annulus and the pressure at both top and bottom of the annulus.

After failure, the top plate on the fixture was cut off and the annulus was re-pressurized. Leak location was noted.

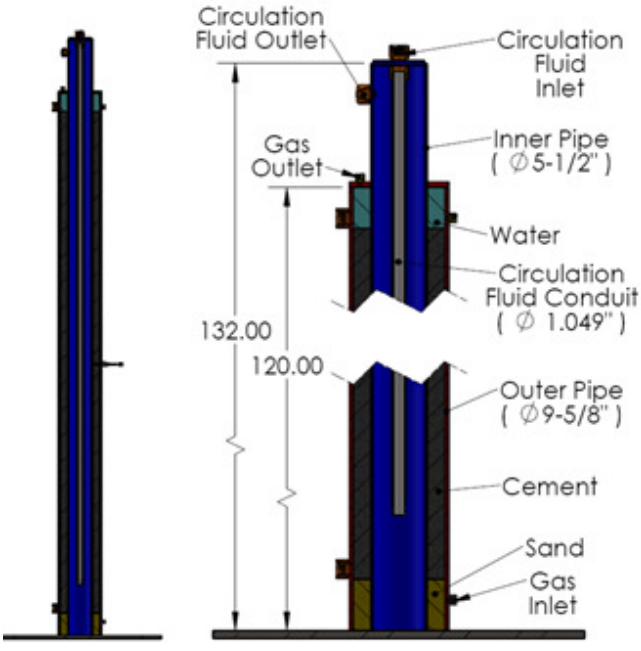

FIGURE 1 LARGE SCALE ANNULAR SEAL TEST (TEMPERATURE)

Testing Methods and Mechanical Properties

Rheology: Slurry surface rheology is measured at ambient temperature with a rotational viscometer. Downhole slurry rheology is measured after conditioning in an atmospheric consistometer if the BHCT is 190°F or less. If the BHCT is greater than 190°F the slurry is conditioned under temperature and pressure in a pressurized consistometer.

API Thickening Time: Slurry thickening time is tested using a pressurized consistometer to simulate downhole pressure and temperature to determine how long the slurry can be pumped before setting.

API Static Fluid Loss: The slurry is conditioned to temperature in an atmospheric consistometer and placed in a fluid loss cell. A 1000 psi differential pressure is applied across the slurry and the amount of fluid released in 30 minutes is recorded. The fluid loss test is a representation of fluid loss from the slurry into the formation during placement.

API Stirred Fluid Loss: The slurry is conditioned at 190□F or above in the fluid loss cell. After conditioning, the cell is rotated and a 1000 psi differential pressure is applied and the amount of fluid released in 30 minutes is recorded.

Free Fluid: A column of slurry is left static at downhole temperature and the volume of free fluid collected at the top of the sample is measured. This is an indication of static slurry stability.

UCA: Compressive strength and time to initial set is measured non-destructively with an Ultrasonic Cement Analyzer (UCA) for 24 hours or 48 hours.

Shearbond: was conducted to measure how tightly the cement is bonded to the central pipe, and was measured by mechanically forcing the inner pipe from a small-scale wellbore model. The simulated formation / cement sheath / central loading tube assembly was placed in a press. The cement and simulated formation was supported while axial load was placed on the central loading tube until movement was detected between the pipe and cement. The load at which this movement occurred was divided by the inner pipe area in contact with the cement to calculate the mechanical shear bond. Figure 2 shows the test schematically.

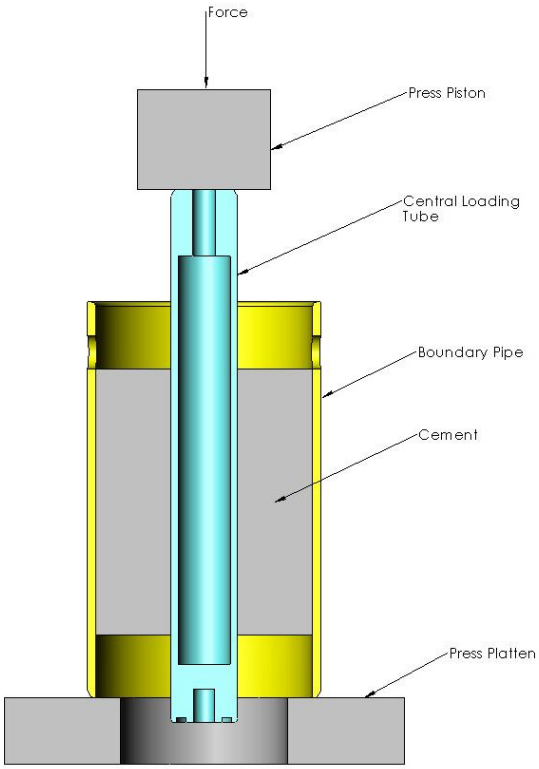

FIGURE 2 SHEAR BOND TEST

Tensile testing was performed using a splitting tensile strength method. For this test, the slurry is cured in a 1.5x5-in mold to make three specimens. After curing, each specimen was prepared by cutting ¼" section from each end. Those pieces were discarded, and the specimen was split into three 1 inch segments specified as top, middle or bottom. Density is then calculated for each segment using Archimedes principle. Each sample is then crushed in the testing apparatus as shown in Figure 3. The maximum reading is noted and used to calculate the tensile strength as per Equation 1.

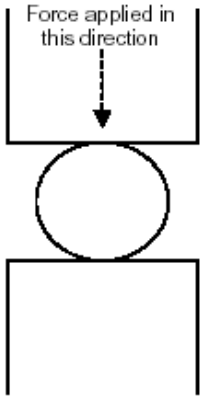

FIGURE 3 DIAGRAM OF TENSILE TEST

Tensile strength is calculated by the following equation:

EQUATION 1 TENSILE STRENGTH EQUATION

$$T\ (psi) = (2*F) / (Pi*L*D)$$

Where:

T = Tensile Strength [psi]

F = Maximum Force Recorded [lbf]

Pi = 3.14

L = Sample Length [in.]

D = Sample diameter [in.]

Impact Resistance: This test consists of repeatedly dropping a steel ball on a cement bar until it breaks. Cement slurry is poured in 5"x1"x1" bar molds and cured at BHST in a water bath for 48 hours. After curing, the slurry bar is placed in the impact test apparatus shown in Figure 4. A 1" ball (66.88 g) is dropped from a constant height on the cement bar. To ensure a consistent point of impact, the ball is dropped through a 1.25" PVC guide pipe placed above the slurry bar. The ball is dropped until the bar breaks, the number of impacts is recorded and used to calculate the energy required to break the bar; this energy is defined as impact resistance of the slurry.

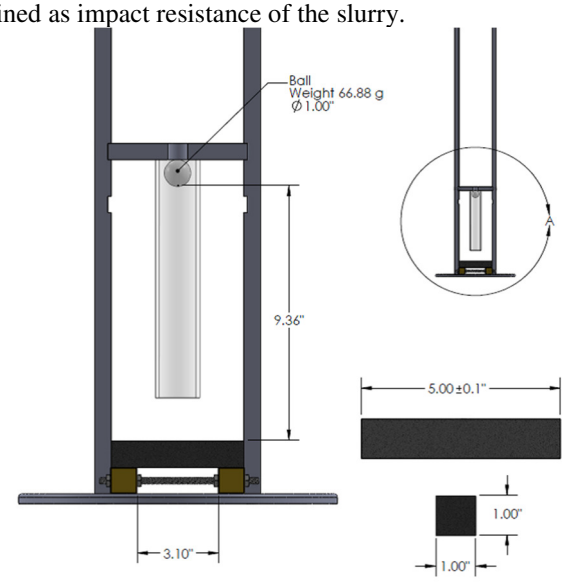

FIGURE 4 IMPACT SETUP

Heat capacity: When heat is transferred to an object, it will cause the temperature of the object to increase. Likewise, when heat is removed, the temperature of the object will decrease. The ratio of heat change to the resulting temperature change is defined as heat capacity. The relationship among the heat (Q) that is transferred, heat capacity (C) and the change in temperature (ΔT) can be summarized as:

$$Q = C*\Delta T$$

Thermal conductivity: When heat is transferred to an object, the rate of transfer across the material is governed by its thermal conductivity. It can be measured by the quantity of heat that passes through an object of known thickness per second.

Coefficient of thermal expansion: During a heat transfer, the volume of the object will change in response of temperature change. Coefficient of thermal expansion is defined by the degree of expansion divided by the change of temperature.

Mechanical Properties of Ultimate compressive strength (UCS), Young's Modulus, Poisson's Ratio, and anelastic strain tests were performed using a standard load frame equipped with LVDT's. Loading for UCS was at a rate of 35psi/sec until failure. To determine Young's Modulus and Poisson's Ratio,

the sample was first loaded to 5% of the UCS, then cycled from 5% to 50% of the UCS for three cycles before ending the test. The sample was fitted with LVDTs to determine radial and axial deformations during loading.

Anelastic strain is a measure of the tendency of cement to permanently deform under less-than-ultimate stress loading. When combined with other mechanical properties, this behavior may explain loss of annular seal in low-intensity loading scenarios. The anelastic strain behavior of oilfield cements mean that the strain response of cement under stress is very non-linear, and that any discussion of Young's (Elastic) Modulus must be tempered with the knowledge that the strict definitions of Elastic Modulus do not apply to oilfield cements.

Coupon Pull Test is a measure of the force required to break the bond between a metal coupon and cement. As seen in Figure 5 a metal coupon is placed in a 2" by 2" metal cylinder and then cemented in place. The coupon is then attached to instrument seen in Figure 6 . This instrument once attached to the coupon can apply force using a torque motor and record the amount of force needed to break the bond. This bond strength is reported in psi.

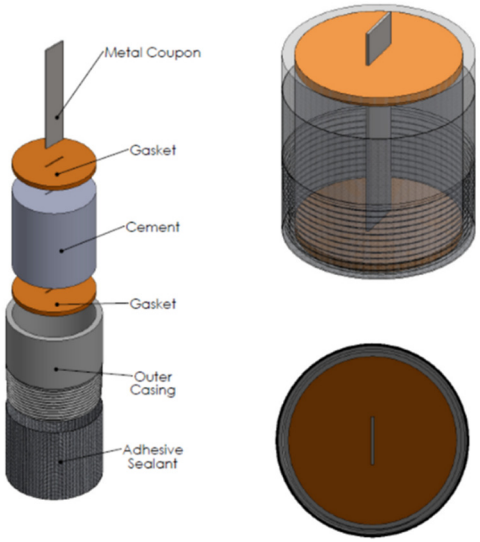

FIGURE 5 COUPON PULL TEST

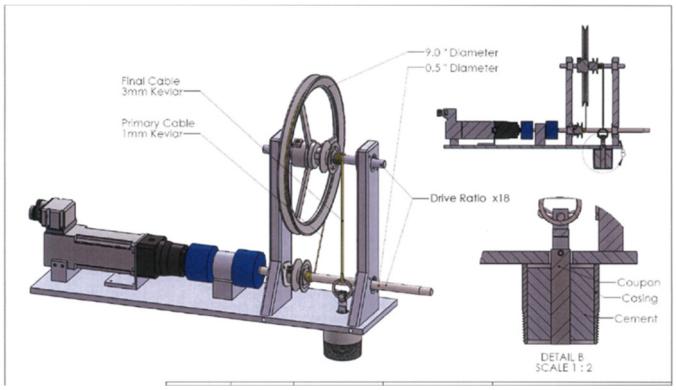

FIGURE 6 TORQUE PULLING DEVICE

Temperature Annular Seal

The Annular Seal Tests were developed in order to measure the ability of cement to maintain an annular seal in a simulated small-scale wellbore. An apparatus as seen in Figure 7 was designed to allow the cement to be stressed by alternately heating and cooling the inner pipe. Various methods were developed to simulate the formation at the outer periphery of the cement sheath. Steel was used to simulate hard formations, and PVC pipe for intermediate to soft-strength formations. These represent the methodology used in the annular seal testing in this project.

Test apparatus and protocols were developed for the thermal loading condition. The apparatus is designed to allow for the application of substantial temperatures.

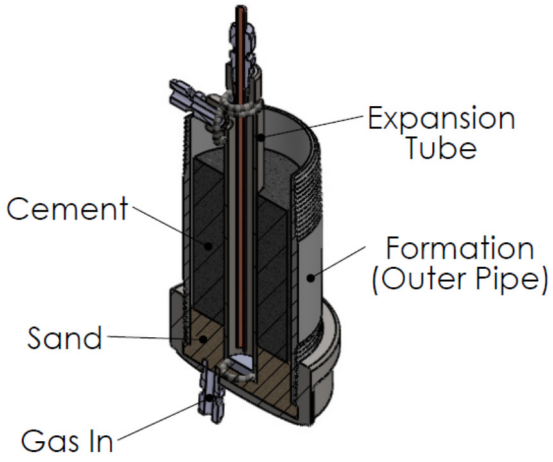

FIGURE 7 THERMAL ANNULAR SEAL APPARATUS

FEA-Model of Lab and Down-Hole System

3D finite element models of the test setups were created using ABAQUS and solved using the explicit solver. The explicit solver was chosen as modeling unreinforced concrete/cement materials can sometimes cause convergence problems in the standard solver due to the extreme non-linearity caused by cracking. The explicit solver is better suited for the analysis of extremely discontinuous events, such as cracking in cement, and can be used to perform quasi-static analyses with complicated contact conditions. Time increments in the Explicit solver are influenced by the overall event time scale, element shape and mass of the system; therefore in order to reduce solve time a combination of mass scaling and reduction of step times were used. To ensure that this method did not influence the solution, energy histories for the systems were checked and the mass scaling used was varied as required.

Geometry of the assemblies was provided by CSI. The small scale assembly is shown in Figure 7 and the large scale assembly is shown in Figure 1.

Where possible, 8 node reduced integration brick elements (C3D8R) were used and are shown in Figure 8. The setup for the large scale lab test was similar and is shown in Figure 9.

The symmetry of the system was taken advantage of in both the small and large scale models. In addition, the coil tubing was modeled to extend just slightly past the faces of the cement sheath to help with model convergence. The sand bed at the bottom of the cement was omitted as it is to allow for the

placement of cement in the pipes and have some compressibility to allow movement. It is not anticipated that the exclusion of the coil tubing ends or the sand bed will have a significant effect on the analysis results.

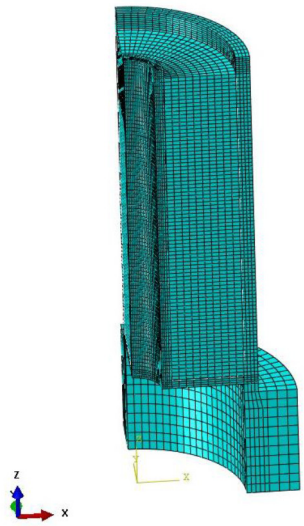

FIGURE 8 SMALL SCALE TEST FIXTURE SHOWING MESH

FIGURE 9 LARGE SCALE TEST FIXTURE SHOWING MESH

Boundary conditions and initial conditions

The small scale large scale models were restrained by fixing the base of the outer pipe in the vertical and horizontal directions. Symmetry planes were used as appropriate. Boundary conditions for the small scale model is shown in Figure 10.

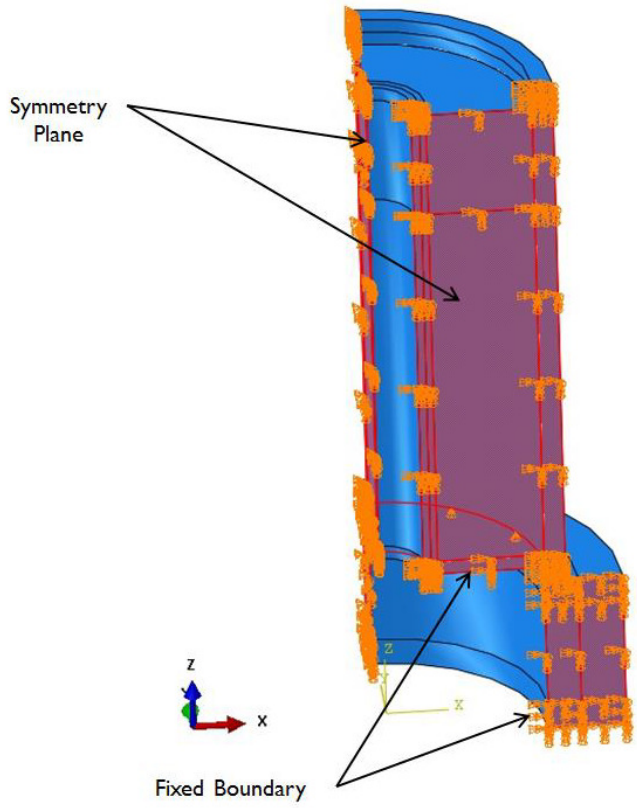

FIGURE 10 BOUNDARY CONDITIONS

Contact Interactions

The test model was treated as an assembly of parts with contact interactions faithfully representing how the parts interact in reality. Surface to surface contact definitions were defined at the cement to coil tubing interface and at the cement to formation pipe interface. The contacts were assigned a cohesive behavior utilizing a traction separation based contact enforcement method. Shear bond strengths at the contacts were determined by CSI.

In order to simulate the de-bonding of the contact surfaces damage initiation was defined using a maximum nominal stress criteria. Once the contact stress reaches the tensile or shear bond strength separation is allowed to begin. After damage is initiated, damage evolution was modeled using a mixed mode fracture energy with exponential softening behavior.

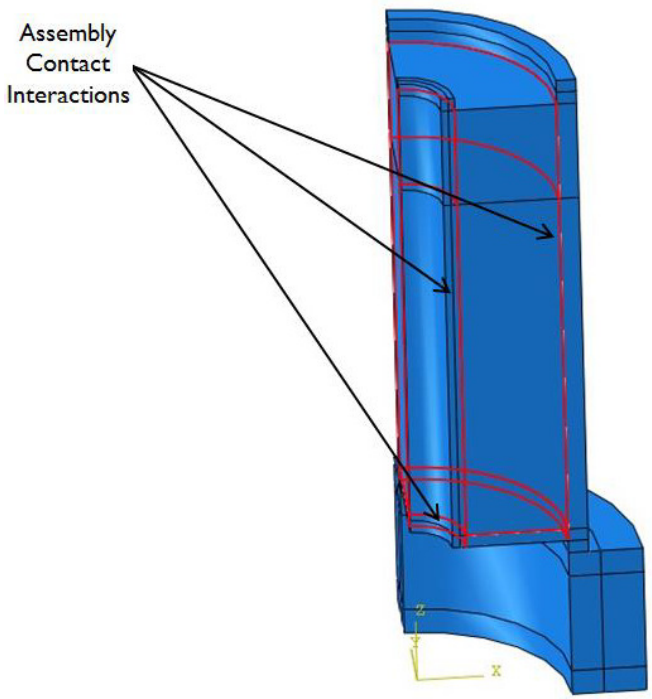

FIGURE 11 TYPICAL CONTACT PAIRS

Figure 11 shows typical contact pairs in the small scale model. It should be noted that the large scale and down-hole system model are similar.

Cement damage modeling

The cement sheaths were modeled using the concrete damaged plasticity model in Abaqus. It provides a general capability for modeling concrete and other quasi-brittle materials in all types of structures by using the concepts of isotropic damaged elasticity in combination with isotropic tensile and compressive plasticity to represent the inelastic behavior of concrete. It consists of the combination of non-associated multi-hardening plasticity and scalar (isotropic) damaged elasticity to describe the irreversible damage that occurs during the cracking process.

The model is a continuum, plasticity-based, damage model for concrete and cements. It is based on the assumption that the main two failure mechanisms are tensile cracking and compressive crushing of the material. The evolution of the failure surface is controlled by two hardening variables, tensile and compressive equivalent plastic strains that are linked to failure mechanisms under tension and compression loading, respectively.

The fracture energy criterion was used to model the cements brittle behavior by using a stress-displacement relationship. The stress-strain behavior of the cement in uniaxial compression outside of the elastic range is modeled by using compression hardening and strain softening.

The concrete compression damage and concrete tension damage optional parameters were used to simulate the loss of stiffness of the cement as damage occurs. Maximum compressive stiffness reduction was set to 99% and 90% for tension. Once these values are reached a complete loss of stiffness is assumed to occur. Element deactivation was enabled to remove these elements from the stiffness matrix at complete failure.

Thermal analysis approach

Thermal loads were applied by means of a sequentially un-coupled thermal stress analysis. To accomplish this, a transient heat transfer analysis was first solved. The nodal temperature values from the heat transfer analysis were then mapped onto the structural solution model. The material definition in the structural model included a thermal expansion coefficient and thus the model developed thermal strains in response to a ΔT and thermal stresses when expansion was resisted by the stiffness of the structure. Since the heat transfer analysis and stress analysis are in different time period thermal properties and convection coefficients were converted into the appropriate time scale.

Heat transfer analyses were performed for the small scale models. To simulate the cycling of cold and hot water, the temperature was varied over time using the load amplitude feature within ABAQUS. A complete thermal cycle consisted of 140°F for 10 minutes and then 38°F for 5 minutes. 325 complete cycles were performed to be imported into the structural model. The initial temperature of the model was assumed to be an ambient temperature of 72°F. The thermal cycling represents the circulation of hot and cold water through the inner pipe in the lab tests.

One heat transfer analysis was performed for the large scale model. The temperature was varied over time using the load amplitude feature within ABAQUS similar to the small scale model. A complete thermal cycle consisted of 150°F for 90 minutes and then 50°F for 90 minutes, 85 complete cycles were performed to be imported into the structural model. The initial temperature of the model was assumed to be an ambient temperature of 72°F. The thermal cycling represents the circulation of hot and cold water through the inner pipe in the lab tests.

One heat transfer analysis was performed for the down-hole system model. An initial temperature of 155°F was assumed down-hole with a temperature of 80°F applied for 180 minutes.

Thermal properties

Thermal expansion coefficient, conductivity and specific heat values for the cement mixes were determined by CSI. In order to reduce computational time, average values of the cement thermal properties were used to reduce the number heat transfer analysis required. A sensitivity check was performed to ensure that this method was an acceptable approach.

The thermal expansion coefficients for the steel pipe and soil were assumed to be typically accepted values.

Thermal boundary conditions

The external boundary conditions were defined by giving the outer surfaces a convection coefficient and a sink temperature (water temperature or ambient air temperature). The circulated water was applied to the interior surface of the inner pipe with a film coefficient. Figure 12 shows an example of the heat transfer analysis performed on the small scale test. The large scale testing was similar.

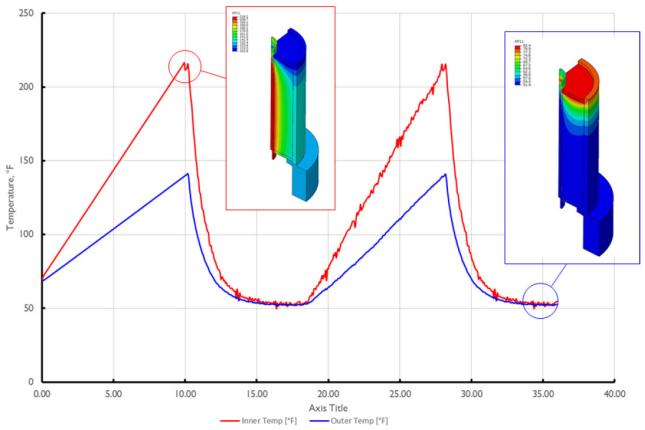

FIGURE 12 HEAT TRANSFER ANALYSIS EXAMPLE

FEA Global Modelling And Tie In FEA Model Data

A finite element model of the full MD of the well bore was constructed, see Figure 13. This took into account all tubular strings from conductor to production tubing along with both liquid and cement filled annuli through the full depth of the well.

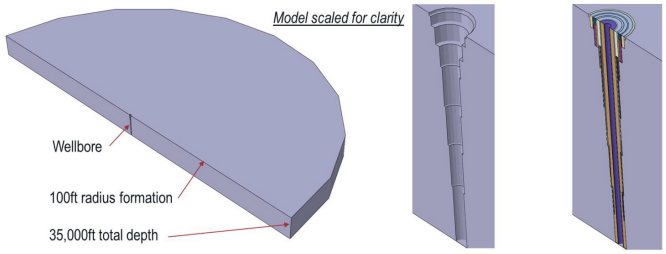

FIGURE 13 FULL WELLBORE MODEL

The individual components were assembled using "hard contact" or tie constraints. De-bonding and micro-annulus cracking were therefore investigated using the individual damage intensities in tension or compression respectively as well as the cracking strains.

The run in and cementing sequence for each tubular was accounted for by performing a series of analysis steps that form the open hole and progressively activates elements representing the tubulars according to the well construction sequence. The cementing process was reflected during the well construction steps in a similar fashion.

Cement was added to the annulus to ensure the string buoyant weight was correct and then either tie constraints or hard contact between the cement and tubulars was activated after the cement placement had occurred.

The analysis included a 20 step process to simulate the well construction phase as follows:

- Step 1 – Geostatic equilibrium of formation
- Step 2 – Remove open hole material
- Step 3 - Run-in conductor
- Step 4 – Cement conductor
- Step 5 – Run-in casing 1
- Step 6 – Cement casing 1
- Step 7 – Run-in casing 2
- Step 8 – Cement casing 2
- Step 9 – Run-in casing 3 / liner
- Step 10 – Cement casing 3
- Step 11 – Run-in casing 4 / liner
- Step 12 – Cement casing 4
- Step 13 – Run-in casing 5
- Step 14 – Cement casing 5
- Step 15 – Run-in casing 6 / liner
- Step 16 – Cement casing 6/liner
- Step 17 – Run-in casing 7
- Step 18 – Cement casing 7
- Step 19 – Run-in production tubing
- Step 20 – Lock production tubing at packer.

Intermediate steps were also included during the cementing process not shown in the above list for analysis control purposes.

The well was modelled as an uncoupled heat transfer problem. The temperature field was calculated without consideration of the stress/deformation of constituent parts of the well, which was reasonable in the context of an oil well as the deformation of the steel tubulars does not alter the heat transfer characteristics of the well.

The FE model also accounted for thermal convection as well as conduction for any fluid filled cavities such as annuli.

Once the well run- in sequence was complete the well was brought onto production and the well warmed up to its steady state production temperature. Thermal shock load cases were then carried out.

Thermal Shock Load Cases:

The entire well structure was initialized with the geostatic temperature profile, in this case assuming a mudline temperature of 40˚F and bottom-hole temperature of 350˚F.

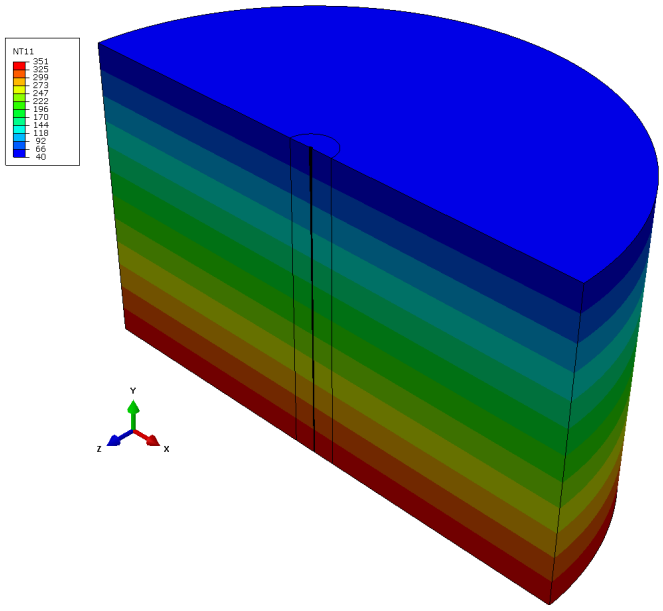

FIGURE 14 INITIAL TEMP PROFILE

Production – bottom hole temperature = 350˚F, well flow rate set as 20,000 bpd. Solved until steady state delivery temperature was reached..

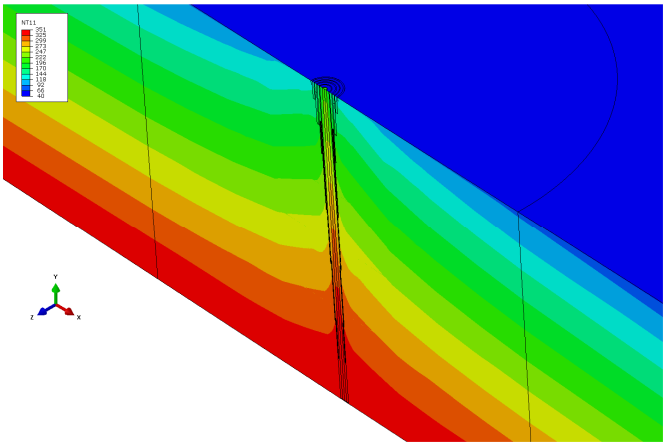

FIGURE 15 PRODUCTION TEMP PROFILE

Shut-in – well flow was halted and the well allowed to cool to 5 days.

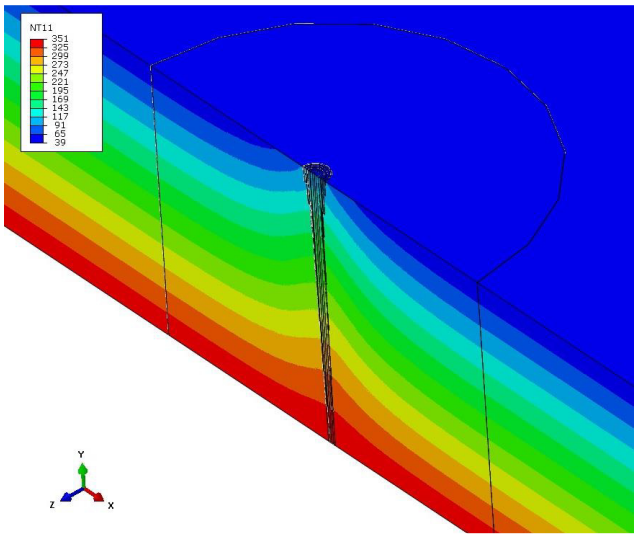

FIGURE 16 SHUT IN TEMP PROFILE AT 5 DAYS

Stimulation – a typical well stimulation profile is shown below.

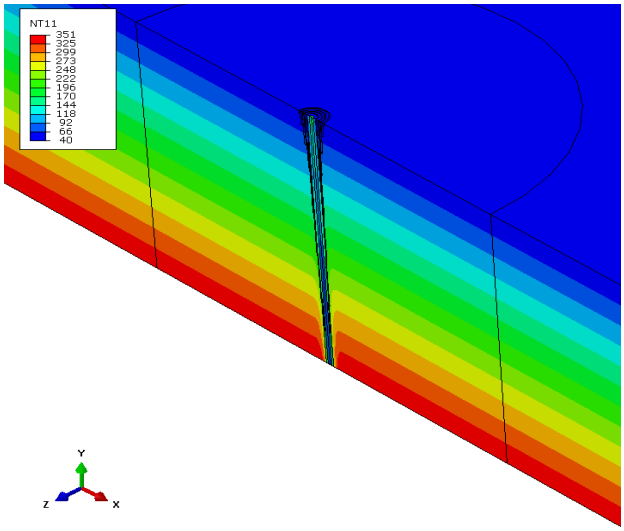

FIGURE 17 WELL STIMULATION TEMPERATURE PROFILE

Thermal Response using FEA model data

The Abaqus FE model that solved the thermal and structural response used a similar finite element mesh, simply swapping heat transfer elements for their structural equivalent. The temperature field from the thermal analysis was mapped onto the structural model and the structural response solved. A nominal annular pressure ranging from 25-250 psi due to the thermal expansion of the annular fluids was also applied. It was assumed that the annular pressure was monitored and managed per API requirements.

The global model also includes damage models for the cement to identify when and where cement damage occurred. These damage models were validated against experiments, see previously mentioned lab testing above.

Results

Cement Failure Modes:

Stresses induced on typical deep-water wells by stimulation operations result from increased casing pressure and thermal cycling of the casing by fracturing fluids. The magnitudes of these stresses are not generally sufficient to be the primary cause of damage to the tubulars. However, the stresses can be sufficient to cause failure of the cement or to destroy the bond of cement to casing or cement to formation. The failure of the cement to casing bond could potentially increase the loading of the casing which in turn could overstress it and lead to a failure.

Potential failure modes of cement from thermal stress during the combination of production-shut in cycles and stimulation can be attributed to tensile stress, compressive stress, and shear stress. The casing-cement-formation system integrity depends on mechanical properties of the cement such as Young's Modulus, Poisson's Ratio, and tensile strength. Cement failure in tension during stimulation is considered very common due to the intrinsically low tensile strength of most Portland cement systems. This can be amplified if the low tensile strength system is has a higher Young's Modulus.

Additionally, the quality of cement placement and control of unwanted fluid migration in the cemented annulus after cement placement dictate the initial condition of the system and affect the potential for stress-induced seal failure. Finally, since Portland cement mechanical properties are governed by extent of chemical hydration occurring in the cement and this hydration rate depends on time, temperature and cement design, the mechanical properties of the cement component must be measured after curing for appropriate times at simulated down-hole conditions to accurately assess performance.

In addition to time dependence, mechanical performance of Portland cement can degrade under cyclic stress that is far below failure stress for the material. This degradation is due to the porous nature of set Portland cement and localized failure of the pore walls that can result from stresses in the elastic region. Thus, stresses lower than failure strength of cement can cause plastic strains. Stress repetition from thermal stress/cycling can result in additional plastic strain thus creating channels that allow flow at lower-stresses.

In general, failure of the casing-cement-formation system as a result of thermal shock-induced stress is complex and is not accurately described by solely one or two cement mechanical properties. Primary failure points are within the cemented

annulus. Failure is governed by cement composition, quality of cement placement, extent of hydration as governed by the time interval between cement placement and stimulation treatment, and stimulation treatment temperatures and pressures.

Mechanical Failure Modes:

In general, a failure to a casing/tubular in the wellbore would occur after a failure or significant damage occurred within the cement annulus. While the design of the tubulars typically does not consider thermal shock explicitly, it is accounted for in the thermal loading applied. If a failure to a tubular is the primary cause of failure in the wellbore, the most likely cause will be due to a failed connection. This type of failure is not typically caused by thermal stress alone, but rather an additional factor such as:

Improper design or exposure to loads exceeding capacity
Failure to comply with make-up requirements
Failure to meet manufacturing tolerances
Damage during storage and handling
Damage during production operations
- e.g., corrosion and wear

Thermal Stress response results

Cement seal failure is not a simple process governed by one or two physical properties. However, the failure trends identified by physical and FEA can be quantified using various groups of cement mechanical and thermal properties, casing and borehole geometry, geothermal conditions, and completion operations. These quantifiable trends present a basis for wellbore design, cement design and placement, and stimulation treatment design. Figure 18 and Figure 20 respectively.

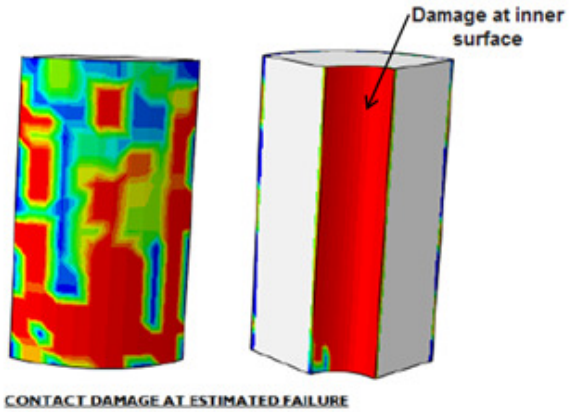

FIGURE 18 SMALL SCALE INNER FAILURE

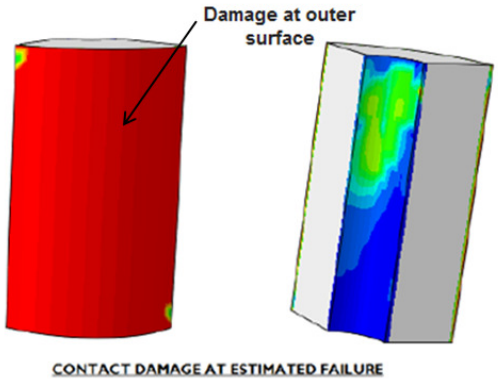

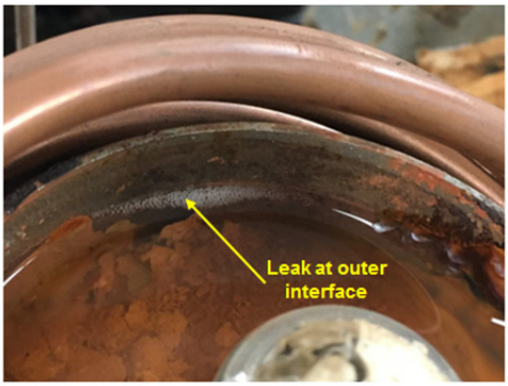

FIGURE 19 SMALL SCALE OUTER FAILURE

TABLE 4 SMALL SCALE LAB VERSUS FEA COMPARISONS

Case	Lab results		FEA Results	
	N_{TEST}	Location	N_{FEA}	Estimated location
Deepwater Shallow Target Low-Density	161	Outer pipe	115	Radial Cracking/Outer
Deepwater Deep Target	338	Inner pipe	>325	None
Deepwater Deep Target	284	Inner pipe	107	Inner Pipe Area
Deepwater Shallow Target Resilient	233	Inner pipe	194	Inner Pipe Area
Deepwater Shallow Target Conventional	218	Inner pipe	124	Inner Pipe Area

Case	Lab results		FEA Results	
Cement 4	70 cycles	Outer pipe	50 cycles	No fail up to 50 cycles[1]
Cement 1	Instant Failure	Inconclusive	1 cycle	Path goes from inner to outer
Cement 5	No Failure	N/A	No Failure	No fail up to 50 cycles
Cement 2	8 cycles	Outer	7 cycles	Path goes from inner to outer
Cement 3	Instant Failure	Inconclusive	2 cycles	Path goes from inner to outer
Cement 6	No Failure	N/A	50 cycles	No fail up to 50 cycles

TABLE 5 LARGE SCALE LAB VERSUS FEA COMPARISONS

Case	Lab results		FEA Results	
Conventional	N_{TEST}	Location	N_{FEA}	Estimated location
Thermal Cycles	31	-	40	Inner Pipe Area/Disking
Thermal Cycles	1-2	Inner and Outer	1-3	Inner Pipe Area/Disking

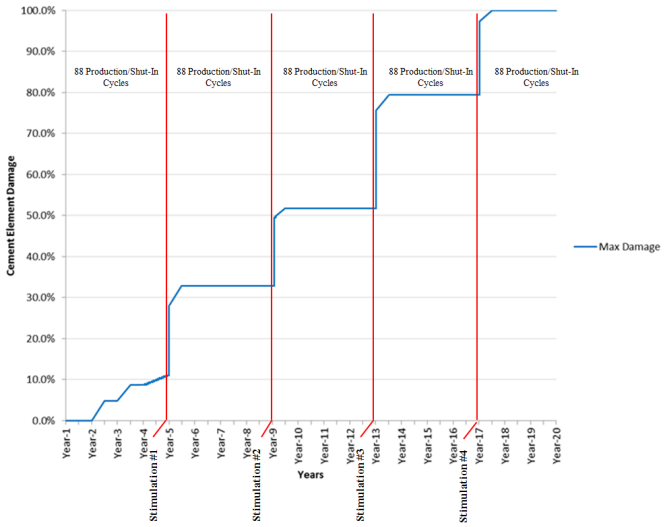

FIGURE 20 DAMAGE CAUSED BY SPECIFIC EVENTS

Another portion of this work was to perform a comparative analysis of the wellbore response when various cements with different material properties were used. It was found that the mixes currently being implemented for TD performed very well. Three mixes of varying properties were used with two being ones suited for TD thermal loading. Third was a mix with lower strengths. It was observed that the mixes with higher qualities perhaps unsurprisingly performed the best. The same mix was used for the entire height of the well. While realizing that this is not typical practice it allows for a comparative assessment. It can be seen that the lower strength cement incurred more damage up the well than the higher strength cements. Figure 21 to

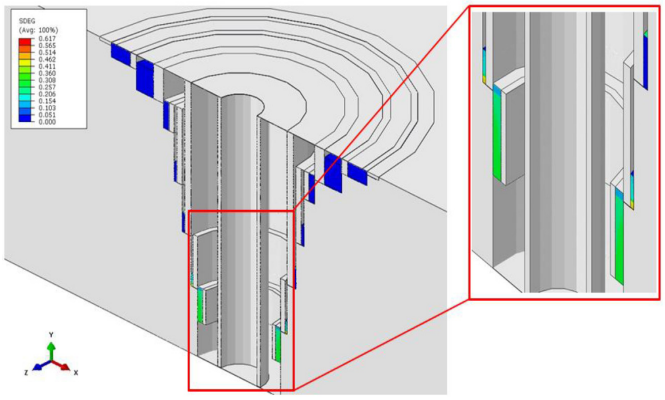

FIGURE 21 LOCAL ELEMENT DMG AFTER 4 STIMULATIONS FOR HDV0965-2C

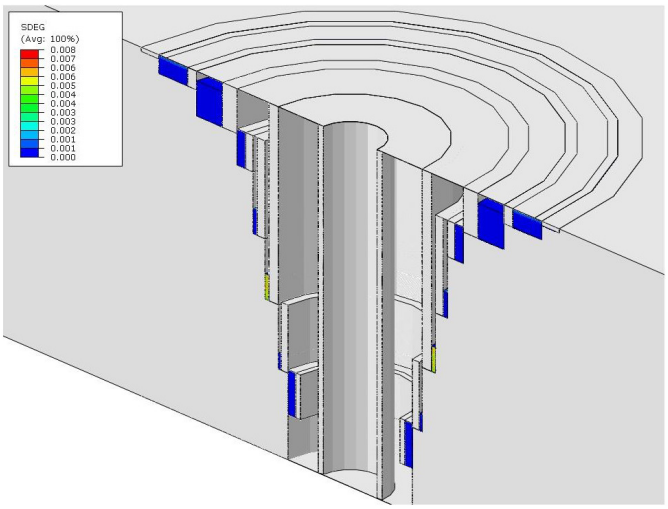

FIGURE 22 LOCAL ELEMENT DMG AFTER 4 STIM FOR D-W DEEP TARGET

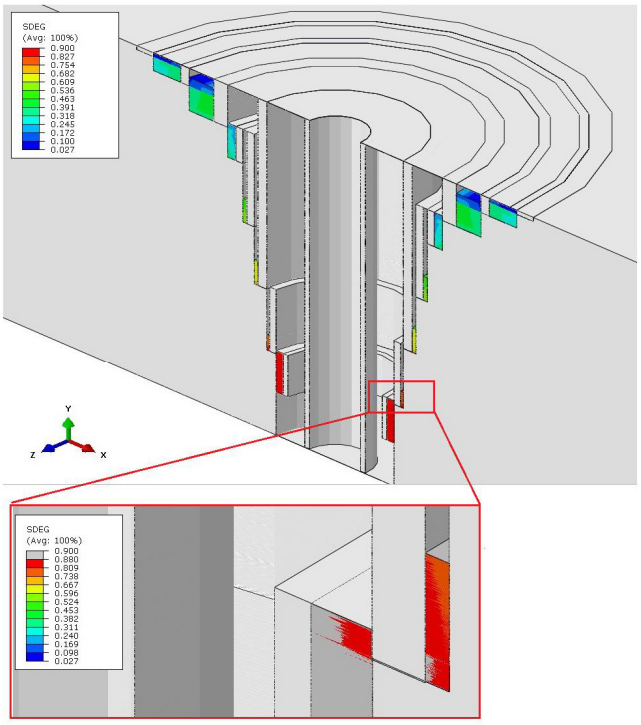

FIGURE 23 LOCAL ELEMENT DMG AFTER 4 STIM FOR HDV0965-1B

Thermal Shock Conclusions

This study of thermal stress in OCS wells amplified and improved understanding of well integrity risk resulting from thermal stress. Thermal gradients resulting from well operations occurring throughout a well's productive life can induce significant stresses in the well-sealant-formation composite system. Magnitudes and rates of application for these stresses varies depending on operation and location in the well, but these stresses can be sufficient to induce seal failure. Tubular failures caused from thermal stresses alone are less likely partly due to the improvements in connection design, although failure could be induced in a weakened tubular area or damaged connection. While thermal stress may be unavoidable in OCS wells, sealants can be designed to minimize potential for seal failure and subsequent uncontrolled fluid movement behind pipe.

The results of a 20yr life cycle case indicate some damage in the lower portions of the cement in the well. However, the damage does not propagate the entire height of the cement column. It was also observed that the magnitude of damage from stimulating the well is much greater than a typical production and shut-in cycle and occurs at the lower end of the well. However the scenario investigated was not intended to cover all the situations that may arise over the life of a well, but rather give insight on the magnitude of damage caused thermal loads on the well and demonstrate that this can be quantified through analysis.

Specific conclusions drawn from this investigation are:

- Physical modeling of sealant failure induced by thermal stress cycles in laboratory scale was matched closely by FEA and indicates that comparative assessments can be made and applied to downhole models.
- Sealant resistance to cyclic thermal stresses is not determined by a single mechanical property. Instead, seal durability appears to be related to a complex interrelationship of mechanical properties including Young's modulus, tensile strength, and water/solids ratio.
- Higher tensile strength increases sealant resistance to thermal shock while increased Young's modulus decreases sealant durability.
- Cements designed to seal across production intervals were most durable sealants (highest resistance to thermal shock) applied in OCS wells. The design to resist thermal shock is just as important up the well as well as at TD.
- Seal integrity along the middle portion of an OCS well can become important if lower flow barriers fail. Improved durability of sealants usually applied in these positions would provide seal back up to unwanted fluid migration if lower barriers fail.

Acknowledgments

Funding for this project was provided by BSEE (Bureau of Safety and Environmental Enforcement. The project was performed by Wild Well Control and CSI Technologies.

Nomenclature

API = *American Petroleum Institute*
BHCT = *Bottom Hole Circulating Temperature*
BHP = *Bottom Hole Pressure*
BHST = *Bottom Hole Static Temperature*
BHT = *Bottom Hole Temperature*
bpm = *Barrels per Minute*
CaBr2 = *Calcium Bromide*
CaCl2 = *Calcium Chloride*
°F = *Degrees Fahrenheit*
ft = *Feet*
gal = *Gallon*
MD = *Measured Depth*
OCS = *Outer Continental Shelf*
OH = *Open Hole*
ppg = *Pounds per Gallon*
psi = *Pounds per square inch*
PVC = *Polyvinyl Chloride*
TVD = *True Vertical Depth*

References

1. Bassett, J., Watters, J., & Sabins, F. (2012). Foculs on Cement Design and Job Execution Increase Success for Shale Cementing Operations. *Americas Unconventional Resources Conference* (p. SPE 155757). Pittsburgh, PA: Society of Petroleum Engineers.
2. Bassett, J., Watters, J., Combs, K., & Nikolaou, M. (2013). Lowering Drilling Cost, Improving Operational Safety, and Reducing Environmental Impact through Zonal Isolation Improvements for Horizontal Wells Drilled int he Marcellus Shale. *Unconventional Resources and Technology Conference* (p. SPE 168847). Denver, CO: Society of Petroleum Engineers.

3. Brufatto, C. et al. From Mud to Cement-Building Gas Wells. Article by Schlumberger in Oilfield Review Autumn 2003.
4. Gill, A. (2018) Thermal Shock Technology. BSEE, Contract number: E16PS0024.
5. Goodwin, K. J. (1990). Cement Sheath Stress Failure . *Annula Technical Conference and Exhibition* (p. SPE 20453). New Orleans, LA: Society of Petroleum Engineers.
6. Jones, P., & Berdine, D. (1940). Oil-Well Cementing. *Drilling and Production Practice*.
7. McDaniel, J., Shadravan, A., & Watters, L. (2014). Cement Sheath Durability: Increasing Cement Sheath Integirty to Reduce Gas Migration in the Marcellus Shale Play. *SPE Hydraulic Fracturing Technology Conference* (p. SPE 168650). The Woodlands, Texas: Society of Petroleum Engineers.
8. Sabins, F. (2004). MMS Project 426 Long Term Integrity of Deepwater Cement Systems Under Stress/Compaction Conditions. Summary Report for MMS.
9. Schmelzl, E., & Daniel Schlosser, D. A. (2014). CTU Deployed Frac Sleeves Benchmark Horizontal Multi Stage Frac Isolation Performance. *SPE Western North America and Rocky Mountain Joint Regional Meeting* (p. SPE169574). Denver, Colorado: The Society of Petroleum Engineers.
10. Sonnier, P. (2015). Well Stimulation Effects on Annular Seal of Production Casing in OCS Oil and Gas Operations. BSEE, Contract number: E14PC00037.